

## Supporting Information

### Crystallization kinetic engineering for growth of thin metal halide perovskite platelets

*Dong Ding,<sup>a</sup> Bo Zhou,<sup>a</sup> Xiaoteng Li,<sup>c</sup> Jiaqi Duan,<sup>a</sup> Kaiyan Wu,<sup>a</sup> Bin Hou,<sup>a</sup> Honglei Fan,<sup>a,b</sup>  
Hongliang Liu,<sup>\*a,b</sup> Lei Jiang<sup>a,d</sup>*

<sup>a</sup> Shandong Laboratory of Advanced Materials and Green Manufacturing at Yantai, Yantai, 264006, P. R. China.

<sup>b</sup> School of Chemistry and Chemical Engineering, Yantai University, Yantai, 264005, P. R. China.

<sup>c</sup> School of Physics and Optoelectronic Engineering, Ludong University, Yantai, 264000, P. R. China.

<sup>d</sup> Technical Institute of Physics and Chemistry, Chinese Academy of Sciences, Beijing, 100190, P. R. China.

## Table of Contents

### *Crystal growth design concept*

Figure S1. Crystal structure and schematic representation of the conversion from $\text{Cs}_3\text{Bi}_2\text{Br}_9$ to $\text{Cs}_2\text{AgBiBr}_6$ .....	2
--	---

### *Characterization of thin $\text{Cs}_3\text{Bi}_2\text{Br}_9$ platelet*

Figure S2. Statistical data of lateral dimension of $\text{Cs}_3\text{Bi}_2\text{Br}_9$ platelet. ....	3
Figure S3. Cross-sectional SEM image of $\text{Cs}_3\text{Bi}_2\text{Br}_9$ platelet.....	4
Figure S4. EDS spectrum of $\text{Cs}_3\text{Bi}_2\text{Br}_9$ platelet. ....	5
Figure S5. Raman spectroscopic spectrum of $\text{Cs}_3\text{Bi}_2\text{Br}_9$ platelet. ....	6
Figure S6. Correlation between crystal dimension of $\text{Cs}_3\text{Bi}_2\text{Br}_9$ platelets and antisolvent ratio in the system. ....	7
Figure S7. Correlation between crystal dimension of $\text{Cs}_3\text{Bi}_2\text{Br}_9$ platelets and antisolvent type in the system. ....	8
Figure S8. Characterization of product by two-step conversion method. ....	9

### *Characterization of thin $\text{Cs}_2\text{AgBiBr}_6$ platelet*

Figure S9. EDS spectrum of $\text{Cs}_2\text{AgBiBr}_6$ platelet. ....	10
Figure S10. Optical image of $\text{Cs}_2\text{AgBiBr}_6$ polyhedrons synthesized by CC method. ....	11
Figure S11. Powder XRD pattern of the synthesized $\text{Cs}_2\text{AgBiBr}_6$ platelets along with the Rietveld refinement. ....	13
Figure S12. XPS survey profile of $\text{Cs}_2\text{AgBiBr}_6$ platelet. ....	13
Figure S13. Low magnification microscope photograph of $\text{Cs}_2\text{AgBiBr}_6$ platelets. ....	14
Figure S14. Raman spectra of $\text{Cs}_2\text{AgBiBr}_6$ platelets. ....	15
Figure S15. XRD pattern of products synthesis by AM-CC method. ....	16
Figure S16. In-situ monitoring crystal growth during AM-CC process.....	17
Figure S17. Growth rate information of $\text{Cs}_3\text{Bi}_2\text{Br}_9$ and $\text{Cs}_2\text{AgBiBr}_6$ .....	18
Figure S18. Color change of $\text{Cs}_2\text{AgBiBr}_6$ single crystal after grinding.....	20
Figure S19. UV-vis absorption spectra of $\text{Cs}_2\text{AgBiBr}_6$ platelets grown by AM-CC with Ag/Bi molar ratios ranging from 0.3 to 1 and $\text{Cs}_2\text{AgBiBr}_6$ polyhedrons grown by the CC method.....	20
Figure S20. Steady-state PL spectra of $\text{Cs}_2\text{AgBiBr}_6$ platelet and polyhedron powders. ....	21
Figure S21. XRD pattern of as-prepared $\text{Cs}_2\text{AgBiBr}_6$ platelets and polyhedrons films.....	22
Figure S22. SEM images of as-prepared $\text{Cs}_2\text{AgBiBr}_6$ polyhedrons and platelets films. ....	23
Figure S23. SEM images of $\text{Cs}_2\text{AgBiBr}_6$ platelets powder (before film formation process) and respective film.....	24
Figure S24. Transient photocurrent response of $\text{Cs}_2\text{AgBiBr}_6$ platelets and polyhedrons films .....	25
Figure S25. The universality of AM-CC synthesis method. ....	26

## Supplementary Figures

### Crystal growth design concept

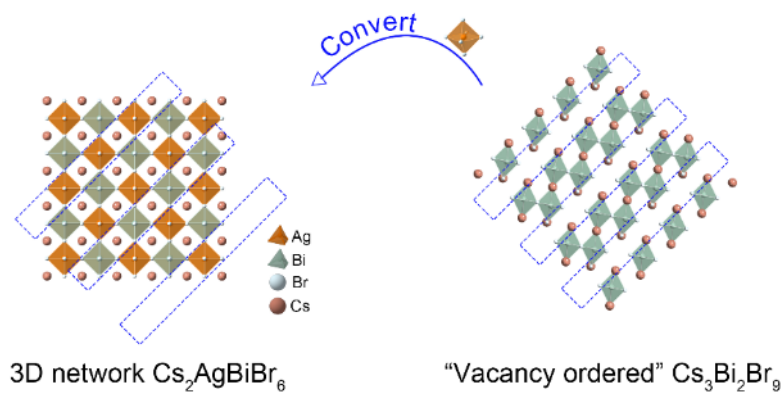


**Figure S1.** Crystal structure and schematic representation of the conversion from  $\text{Cs}_3\text{Bi}_2\text{Br}_9$  to  $\text{Cs}_2\text{AgBiBr}_6$ . Owing to the similar crystal structure between  $\text{Cs}_2\text{AgBiBr}_6$  and  $\text{Cs}_3\text{Bi}_2\text{Br}_9$ , vacancy ordered  $\text{Cs}_3\text{Bi}_2\text{Br}_9$  can be converted into 3D network  $\text{Cs}_2\text{AgBiBr}_6$  by mixing with  $\text{Ag}^+$ , wherein  $[\text{AgBr}_6]^{5-}$  will fill in the "vacancy" sites of  $\text{Cs}_3\text{Bi}_2\text{Br}_9$  and form  $\text{Cs}_2\text{AgBiBr}_6$ .

## Characterization of thin $\text{Cs}_3\text{Bi}_2\text{Br}_9$ platelet

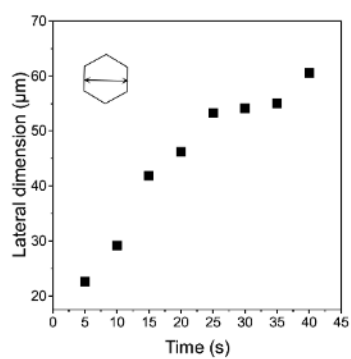


**Figure S2.** Statistical data of lateral dimension of  $\text{Cs}_3\text{Bi}_2\text{Br}_9$  platelet.

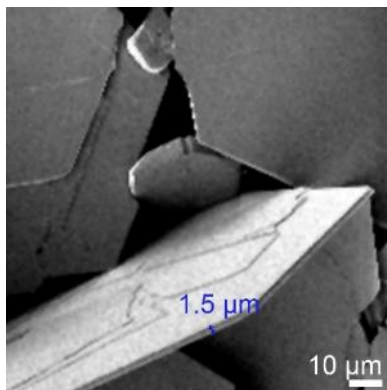


**Figure S3.** Cross-sectional SEM image of Cs<sub>3</sub>Bi<sub>2</sub>Br<sub>9</sub> platelet.

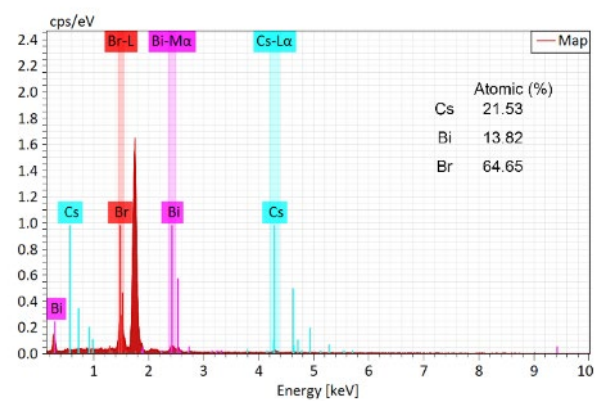


**Figure S4.** EDS spectrum of Cs<sub>3</sub>Bi<sub>2</sub>Br<sub>9</sub> platelet.

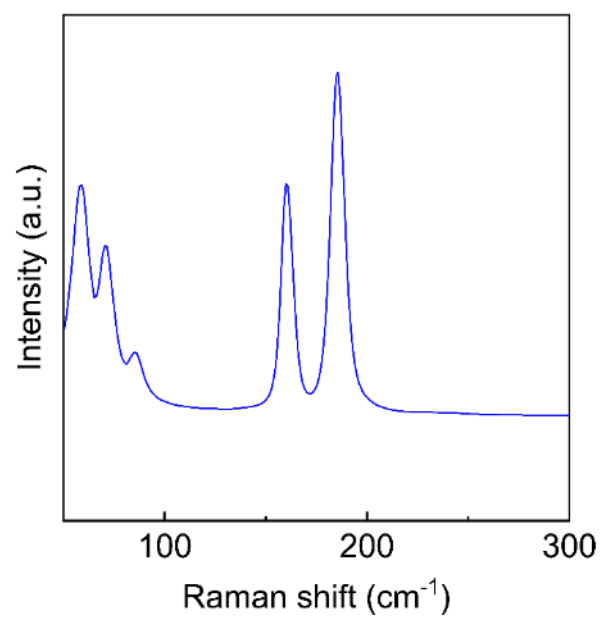


**Figure S5.** Raman spectroscopic spectrum of Cs<sub>3</sub>Bi<sub>2</sub>Br<sub>9</sub> platelet.

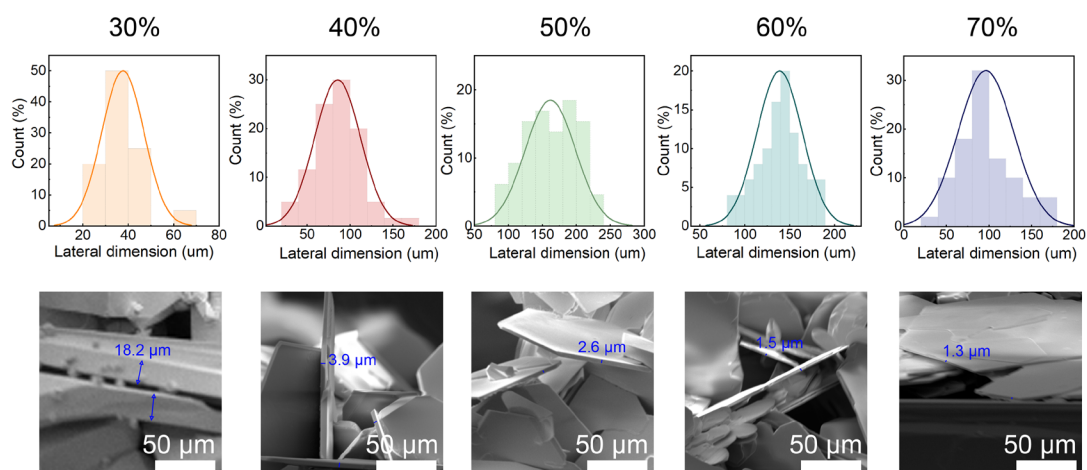


**Figure S6.** Correlation between crystal dimension of  $\text{Cs}_3\text{Bi}_2\text{Br}_9$  platelets and antisolvent ratio in the system. Lateral dimensions and cross-sectional SEM images of  $\text{Cs}_3\text{Bi}_2\text{Br}_9$  platelets grown by AM-CC method using various anti-solvents ratios from 30% to 70%.



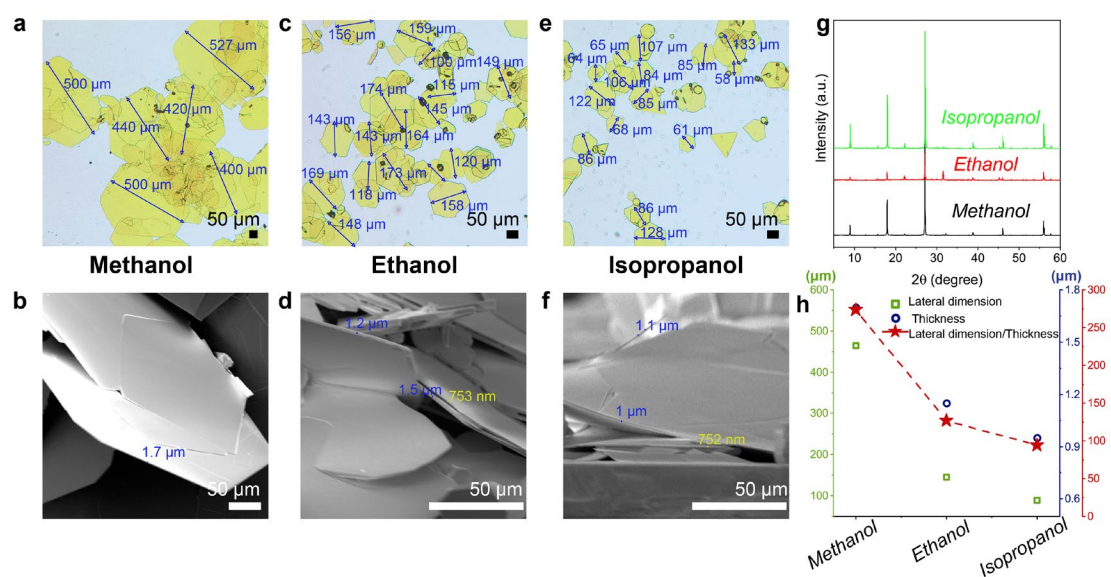


**Figure S7.** Correlation between crystal dimension of  $\text{Cs}_3\text{Bi}_2\text{Br}_9$  platelets and antisolvent type in the system. (a-f) Optical and SEM images of  $\text{Cs}_3\text{Bi}_2\text{Br}_9$  platelets grown by AM-CC method using various anti-solvents including methanol, ethanol and isopropanol, respectively. (g) XRD pattern of as-prepared  $\text{Cs}_3\text{Bi}_2\text{Br}_9$  platelets. (h) Average lateral dimensions, average thickness and lateral dimension/ thickness ratios of as-prepared  $\text{Cs}_3\text{Bi}_2\text{Br}_9$  platelets.

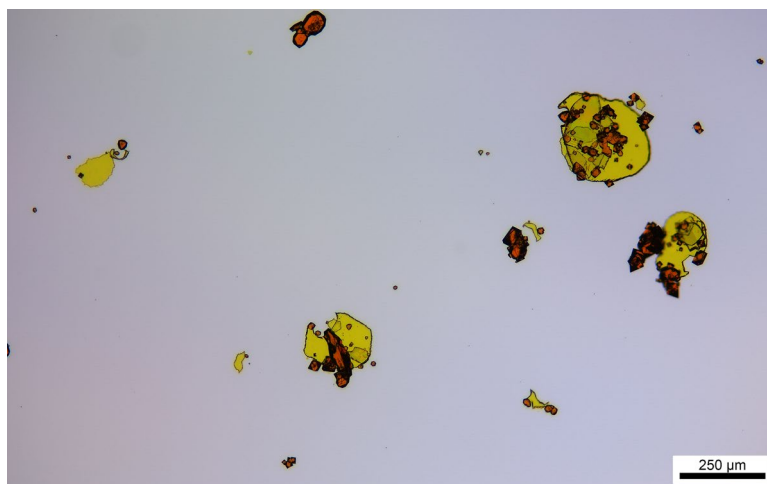


**Figure S8.** Characterization of product by two-step conversion method. Optical image of final product from two-step synthesis method, where  $\text{Cs}_3\text{Bi}_2\text{Br}_9$  platelets were synthesized by AM-CC method, then the  $\text{Cs}_3\text{Bi}_2\text{Br}_9$  platelets were immersed into solution containing AgBr for 1 h.

## Characterization of thin $\text{Cs}_2\text{AgBiBr}_6$ platelet

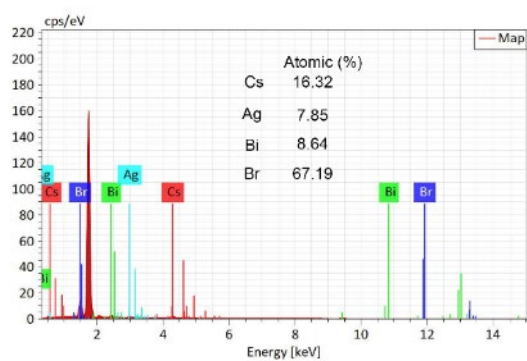


**Figure S9.** EDS spectrum of  $\text{Cs}_2\text{AgBiBr}_6$  platelet.

*Cs<sub>2</sub>AgBiBr<sub>6</sub> polyhedrons (CC method)*

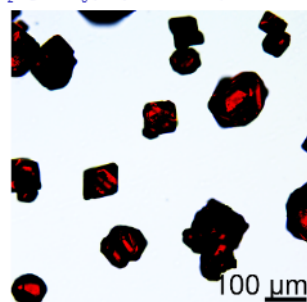


**Figure S10.** Optical image of Cs<sub>2</sub>AgBiBr<sub>6</sub> polyhedrons synthesized by CC method.

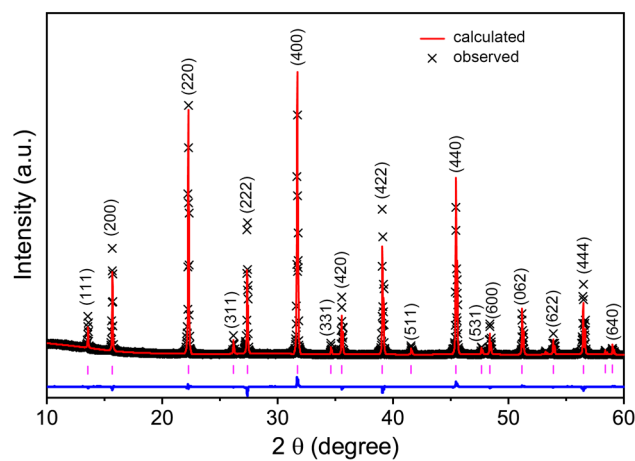


**Figure S11.** Powder XRD pattern of the synthesized  $\text{Cs}_2\text{AgBiBr}_6$  platelets along with the Rietveld refinement.

**Table S1** Main parameters of refinement.

Compound	$\text{Cs}_2\text{AgBiBr}_6$
Phase	Cubic
Sp. gr.	$Fm-3m$
$a$	11.27 Å
$b$	11.27 Å
$c$	11.27 Å
$\alpha$	90°
$\beta$	90°
$\gamma$	90°

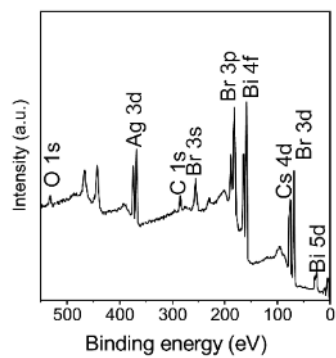


**Figure S12.** XPS survey profile of Cs<sub>2</sub>AgBiBr<sub>6</sub> platelet.

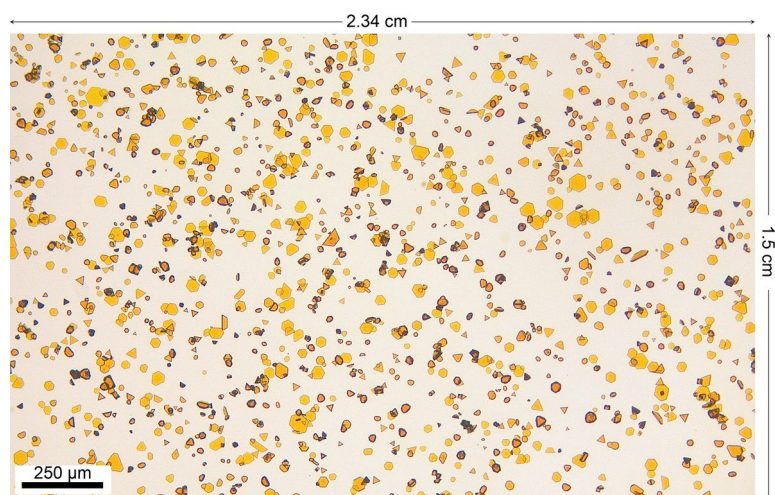


**Figure S13.** Low magnification microscope photograph of  $\text{Cs}_2\text{AgBiBr}_6$  platelets.

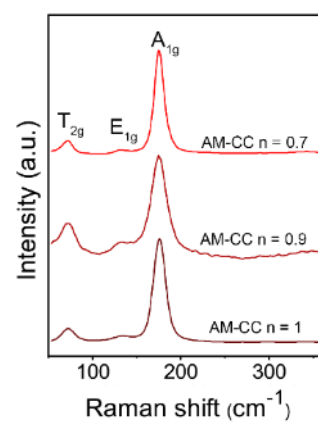


**Figure S14.** Raman spectra of Cs<sub>2</sub>AgBiBr<sub>6</sub> platelets.



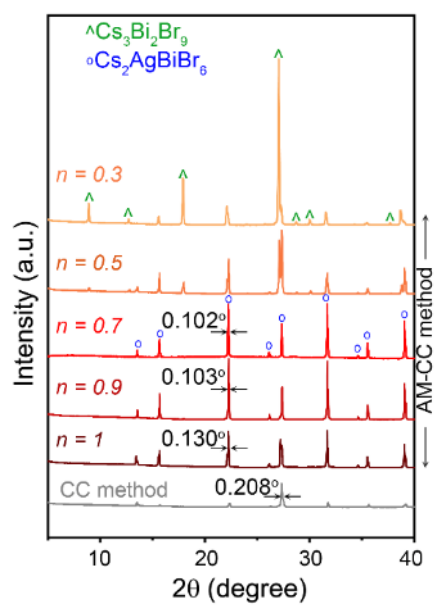


**Figure S15.** XRD pattern of products synthesis by AM-CC method with Ag/Bi molar ratio of 0.3-1.

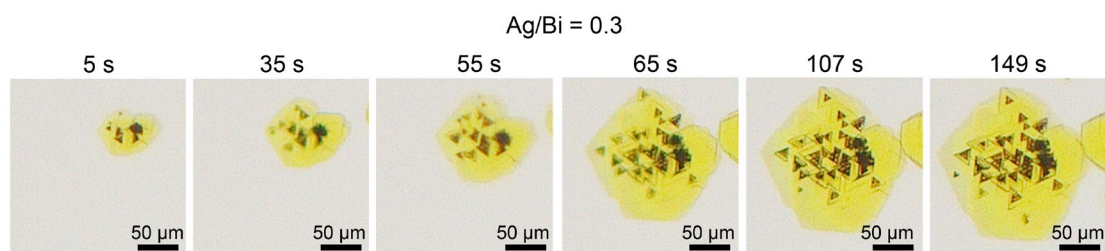


**Figure S16.** In-situ monitoring crystal growth during AM-CC process. The Ag/Bi molar ratio is 0.3.

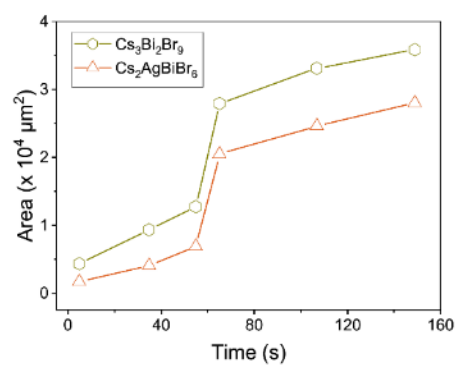


**Figure S17.** Growth rate information of  $\text{Cs}_3\text{Bi}_2\text{Br}_9$  and  $\text{Cs}_2\text{AgBiBr}_6$ . Crystal areas of golden green  $\text{Cs}_3\text{Bi}_2\text{Br}_9$  and orange  $\text{Cs}_2\text{AgBiBr}_6$  as time extends.

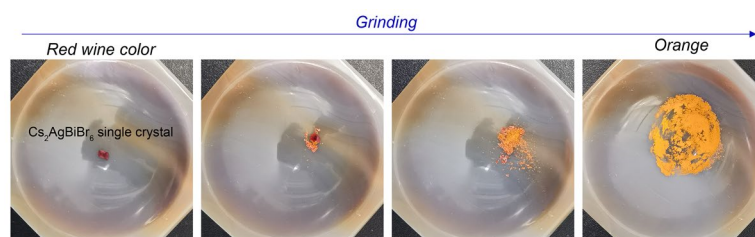


**Figure S18.** Color change of  $\text{Cs}_2\text{AgBiBr}_6$  single crystal after grinding. Photos of pristine bulk  $\text{Cs}_2\text{AgBiBr}_6$  single crystal and its photos with the extension of grinding time. The color changes from red wine to orange as grinding time extends.

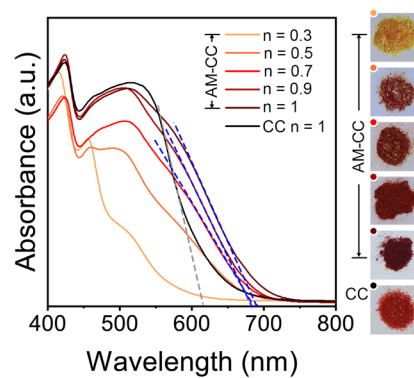


**Figure S19.** UV-vis absorption spectra of  $\text{Cs}_2\text{AgBiBr}_6$  platelets grown by AM-CC with Ag/Bi molar ratios ranging from 0.3 to 1 and  $\text{Cs}_2\text{AgBiBr}_6$  polyhedrons grown by the CC method; the insets show corresponding photographs of the products.

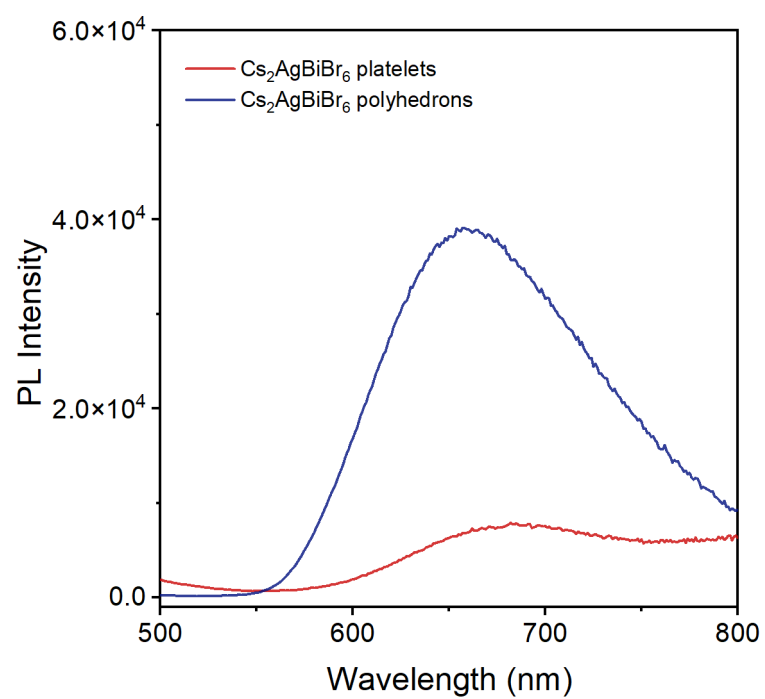


**Figure S20.** Steady-state PL spectra of  $\text{Cs}_2\text{AgBiBr}_6$  platelet and polyhedron powders.

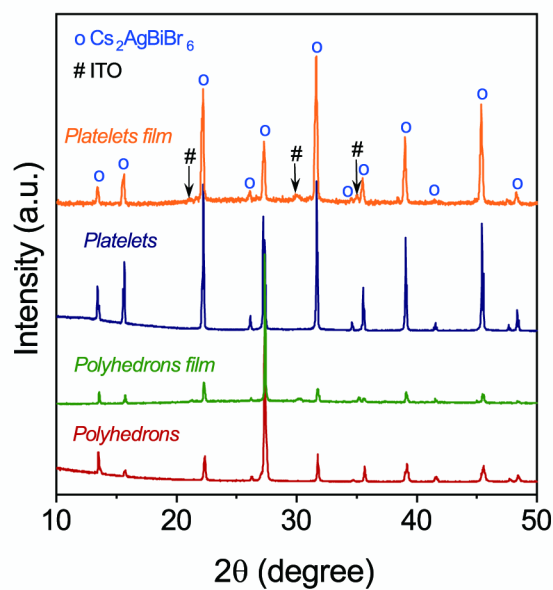


**Figure S21.** XRD pattern of as-prepared  $\text{Cs}_2\text{AgBiBr}_6$  platelets and polyhedrons films.

Figure S21 presents the XRD pattern of as-prepared  $\text{Cs}_2\text{AgBiBr}_6$  platelets and polyhedrons films, all diffraction peaks can be assigned to the characteristic patterns of  $\text{Cs}_2\text{AgBiBr}_6$  (marked with “o”) and ITO glass (marked with “#”), confirming the successful synthesis of pure-phase  $\text{Cs}_2\text{AgBiBr}_6$  platelets and polyhedrons films through this method.

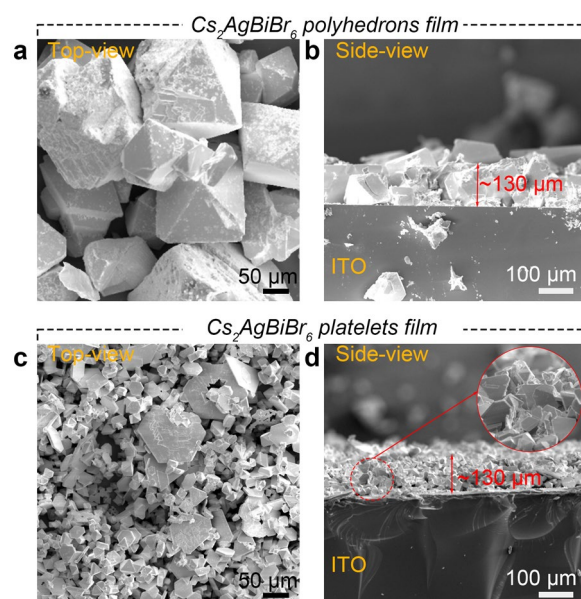


**Figure S22.** Top-view and side-view SEM images of as-prepared  $\text{Cs}_2\text{AgBiBr}_6$  polyhedrons (a-b) and platelets (c-d) films.

Figure S22 shows the SEM images of  $\text{Cs}_2\text{AgBiBr}_6$  platelets and polyhedrons films, as viewed from the top and side, respectively. It is observed that the  $\text{Cs}_2\text{AgBiBr}_6$  platelets and polyhedrons are uniformly dispersed within the film with a similar thickness of  $\sim 130\text{ }\mu\text{m}$ .



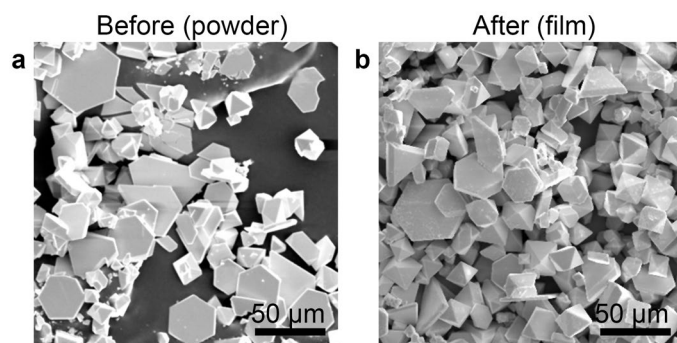


**Figure S23.** SEM images of  $\text{Cs}_2\text{AgBiBr}_6$  platelets powder (before film formation process) and respective film.

We have examined the morphology of the  $\text{Cs}_2\text{AgBiBr}_6$  platelets before and after film preparation, with the corresponding images presented in Figure S23. It is evident that the hexagonal shaped  $\text{Cs}_2\text{AgBiBr}_6$  platelets were well preserved after film formation.

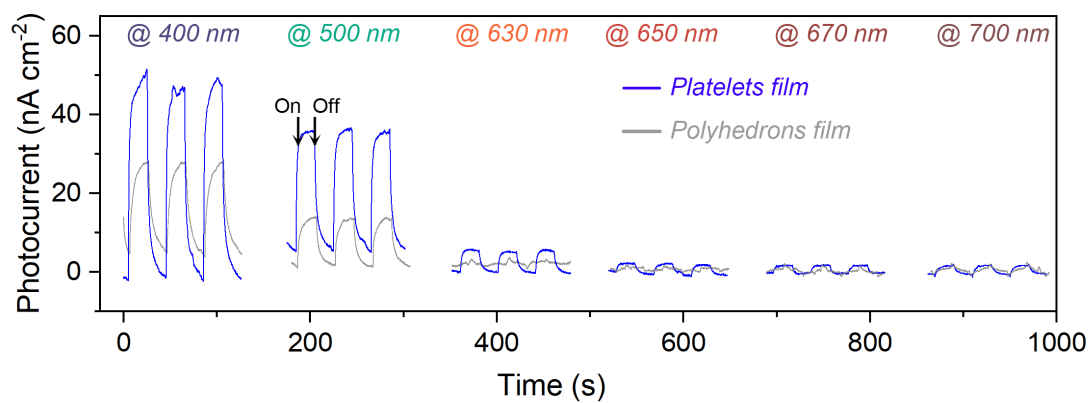


**Figure S24.** Transient photocurrent response of  $\text{Cs}_2\text{AgBiBr}_6$  platelets and polyhedrons films under illumination at 400-700 nm.

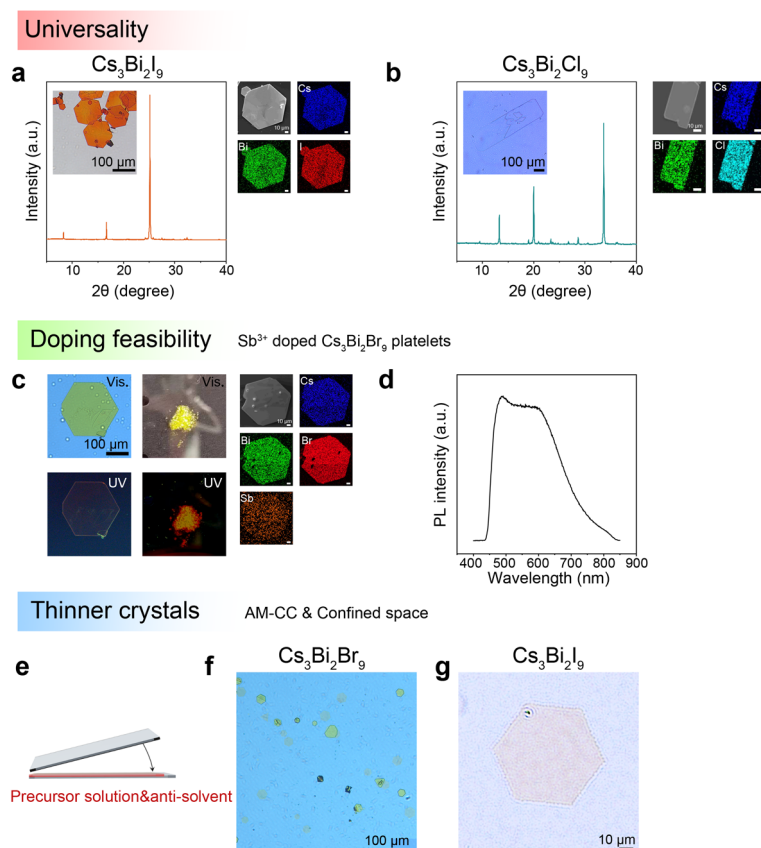


**Figure S25.** The universality of AM-CC synthesis method. (a-b) Optical images and XRD pattern of thin  $\text{Cs}_3\text{Bi}_2\text{I}_9$  and  $\text{Cs}_3\text{Bi}_2\text{Cl}_9$  platelets synthesized by AM-CC method, where  $\text{CsX}$  ( $\text{X}=\text{I}$  or  $\text{Cl}$ ) was added into hot  $\text{HI}$  or  $\text{HCl}$ , and alcohol containing  $\text{BiX}_3$  (molar ratio of  $\text{CsX}:\text{BiX}_3$  is 3:2) was injected into the precursor solution during cooling. (c) Optical images under visible and UV light and (d) PL spectrum of  $\text{Sb}^{3+}$  doped  $\text{Cs}_3\text{Bi}_2\text{Br}_9$  platelets.  $\text{Sb}^{3+}$  doped  $\text{Cs}_3\text{Bi}_2\text{Br}_9$  platelets were grown by adding 5 % (mol)  $\text{SbBr}_3$  into the precursor solution during AM-CC. (e-g) Optical images of ultrathin  $\text{Cs}_3\text{Bi}_2\text{Br}_9$  and  $\text{Cs}_3\text{Bi}_2\text{I}_9$  platelets synthesized by AM-CC combined with confined space, precursor solution containing alcohol were dropped into gaps between two glasses.